

## Technique to reduce multipath GPS signals

B. Rama Krishna Rao<sup>1</sup>, A. D. Sarma<sup>2,\*</sup> and Y. Ravi Kumar<sup>1</sup>

<sup>1</sup>Defence Electronics Research Laboratory, Antenna Division, Hyderabad 500 005, India

<sup>2</sup>R&T Unit for Navigational Electronics, Osmania University, Hyderabad 500 007, India

**It is well known that multipath error is one of the major error sources affecting the positional accuracy of Global Positioning System (GPS). Although the multipath effect can be reduced by choosing sites without multipath reflectors or using proper antennas to mitigate the reflected signal, it is difficult to eliminate all multipath effects from GPS observations. Here, a technique based on vertical ground planes to effectively reduce the multipath occurring at  $\pm 5^\circ$  of the horizon is presented.**

**Keywords:** Antenna, GPS, multipath effects, radomes, satellites.

GLOBAL Positioning System (GPS) is a satellite-based navigation system designed and developed by US Department of Defence (DoD) to provide instantaneous 3D position, velocity and time information almost anywhere on or above the surface of the earth at any time, and in any weather<sup>1</sup>. The GPS receives right-hand, circularly polarized signals from a number of satellites. The circularly polarized signals facilitate the rejection of multipath signals, which can reach the antenna in opposite sense of polarization (left-hand circularly polarized) for which the system will not respond. The design of the antenna is one of the most important aspects in the receiver design. The antenna is expected to cover uniformly all the satellites over the hemisphere, with high rejection of the multipath and cross-polarized signals and a radiation pattern with a sharp roll-off at low elevation angles near the horizon<sup>2</sup>. Majority of the current GPS receivers operate at  $L_1$  (1575.42 MHz) and  $L_2$  (1227.6 MHz) frequencies and use right circularly polarized microstrip patch antennas due to their compact size and low cost when compared to choke ring antenna. The disadvantage of microstrip antenna is that it cannot reject multipath signals. Therefore, multipath-resistant GPS receiving microstrip antennas are designed with ground planes to reject the radio waves arriving through multipath at low elevation angles near the horizon. To protect the antenna from environmental extremities, radomes are also designed and developed. The details of design, development of antennas with ground planes and radomes are presented here.

The positional accuracy provided by GPS is limited by

various errors. Also, the GPS pseudorange obtained by either carrier-phase or code-phase measurements is affected by several types of random errors and biases (systematic errors). These errors can be classified as those originating at the satellites, those originating at the receiver and those that are due to signal propagation<sup>1</sup>. Errors originating at the satellites include orbital errors, satellite clock errors, and the effect of anti-spoofing (AS). Errors originating at the receiver include receiver clock errors, multipath errors and receiver noise and antenna phase centre variations. The signal propagation errors include delays of the GPS signal as it passes through the ionospheric and tropospheric layers of the atmosphere. In addition to the effect of these errors, the accuracy of the computed GPS position is also affected by geometric locations of the GPS satellites as seen by the receiver. The more spread out the satellites are in the sky, better is the accuracy. With the use of differential techniques it is possible to remove many of the common-mode error sources, but the error effects of multipath have proven much more difficult to mitigate.

Multipath is the phenomenon by which the GPS signal is reflected by some object or surface before being detected by the antenna. Multipath is more commonly considered to be the reflections due to surfaces surrounding the antenna and can cause a range of errors as high as 15 cm for the  $L_1$  carrier and of the order of 15–20 m for the pseudoranges<sup>2</sup>. By proper siting and antenna selection, the net impact of multipath is less than 1 m under most circumstances. A typical multipath scenario is presented in Figure 1. Multipath signals are characterized by four parameters and all are relative to the direct line-of-sight signals. These are amplitude, time delay, phase and phase rate of change. The relative phase is a function of the additional path length and the electrical properties of the reflecting/diffracting medium, while the phase rate of change accounts for the changing multipath propagation environment due to the relative satellite-user dynamics<sup>1</sup>.

Multipath effects can be reduced to some extent by choosing a proper antenna and its location without multipath reflectors. Pasetti and Glulicchi<sup>3</sup> discussed three multipath mitigation techniques. The first technique uses look-up table that stores the expected multipath error as a function of azimuth and elevation angles of the incoming GPS

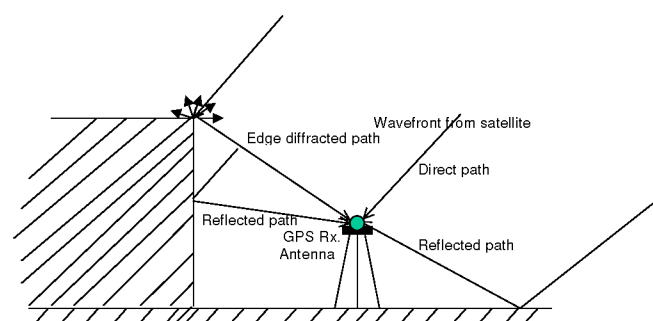


Figure 1. Typical multipath scenario.

\*For correspondence. (e-mail: ad\_sarma@yahoo.com)

signal. In the second technique the Kalman filter is used to remove multipath component and in the third technique signal-to-noise ratio component is used to compensate multipath effects. However, our work is focused on multipath mitigation using hardware aspects. Multipath can be improved by brute-force method of putting a large ground plane around the antenna<sup>4</sup>. However, it is impractical, since the large ground plane increases the weight and size of the antenna. Use of tuned or un-tuned microwave absorbers around the antenna can avoid multipath signals to some extent, but the absorbers may not withstand adverse weather conditions. Reactive surfaces of concentric choke rings also help mitigate multipath effects, but in this method also the weight of the antenna is more. Even though these techniques have both advantages and disadvantages, they are used for multipath signal rejection by the antenna only through low elevation angles below the horizon<sup>4</sup>. But multipath rejection is required for small elevation angles both above and below the horizon of the antenna. Most of the multipath signals will enter the antenna through small elevation angles near the horizon. Hence, there is a need to develop multipath-resistant antennas with multipath rejection from small elevation angles (i.e. +5° to -5°) above and below the horizon.

To make GPS more accurate and effective, a high-level performance from each component is aimed, especially from the antennas. The space segment antennas should have a shaped pattern beaming towards the earth to cover the particular surface area. The control segment antennas should have high gain and low noise characteristics<sup>1</sup>. Antennas for GPS user segment are required to receive right-handed circularly polarized signals from all the visible satellites over the hemisphere. The receiving antenna should have cross-polarization component of the order 15 dB to reject multipath and cross-polarized signals<sup>4</sup>. Furthermore, as the signal received by the antenna is weak, the impedance matching is an important aspect as well as the possibility of operation at the two frequencies, i.e. L<sub>1</sub> (1227.6 MHz) and L<sub>2</sub> (1575.42 MHz). The roll-off at low elevation angles should be high<sup>4</sup>, to reject the multipath signals at these angles. Thus, GPS antennas are more difficult to design compared to various other antennas in common use like TV and radio antennas. Mechanical requirements like size, weight, profile, etc. make significant impact on the antenna configuration. Also, environment factors play an important role. The importance of these factors varies depending upon the location of the antenna. The process of fabrication and material should be such that a high degree of uniformity and repeatability exists between the units.

Taking the antenna requirements into consideration, two circular patch antennas at L<sub>1</sub> and L<sub>2</sub> frequencies were designed with vertical ground planes. The antennas with vertical ground planes were protected from environmental extremities with thin-wall Glass Fibre-Reinforced Plastic (GFRP) hemispherical radomes. The heights of the ground planes and diameters of the radomes for the two antennas

are determined by considering the required radiation pattern of the antenna and cut-off angles for multipath rejection.

The elliptical polarized signals are defined by three parameters, i.e. axial ratio, tilt angle and sense of rotation. If axial ratio is zero or infinity, polarization becomes linear (zero for horizontal and infinity for vertical). When axial ratio is unity, it becomes a perfect circular polarization. In case of linear polarization sense of rotation is not applicable, whereas in circular polarization tilt angle is not applicable. In the case of circular polarization, axial ratio will determine the quality of circularity. Patch antennas are resonant-type of antennas and radiate linear polarized signals<sup>5</sup>. Single patch antenna can be made to radiate circular polarized signal, if two orthogonal mode signals are excited simultaneously with equal amplitudes and ±90° out of phase with sign determining the sense of rotation. One of the methods for achieving these conditions slightly perturbs the patch at appropriate locations with respect to feed location<sup>6</sup>. A standard circular patch antenna and single-fed circular polarized patch antenna are shown in Figure 2 a and b respectively. A single-point feed patch capable of producing CP radiation is desirable in situations where it is difficult to accommodate dual orthogonal feeds with a power divider network. The feed point is always located diagonal with respect to the perturbation segments of ΔS of the circular patch of area S (Figure 2 b). The feeding arrangement of the circular patch antenna is shown in Figure 2 c. For circular polarization, the radiation condition is<sup>6</sup>,

$$\left| \frac{\Delta S}{S} \right| = \frac{1}{1.841Q_0}, \quad (1)$$

where Q<sub>0</sub> is unloaded ‘Q’ factor of the circular patch.

The resonance condition corresponding to the zeros of the derivative of Bessel function is

$$J_n^1(k_0 a \sqrt{\epsilon_r}) = 0. \quad (2)$$

For the lower-order mode, n = 1, the first root of J<sub>1</sub><sup>1</sup>(.) occurs at 1.841, thus

$$k_0 a \sqrt{\epsilon_r} = 1.841. \quad (3)$$

Due to the fringing fields at the periphery of the disc conductor, a becomes a<sub>e</sub>. A disc with physical radius a has an effective radius a<sub>e</sub> such that a<sub>e</sub> > a. The semi-empirical relationship between a and a<sub>e</sub> is given by<sup>6</sup>

$$a_e = a \left[ 1 + \frac{2h}{\pi a \epsilon_r} \left( \ln \frac{\pi a}{2h} + 1.7726 \right) \right]^{\frac{1}{2}}. \quad (4)$$

Therefore, eq. (3) can be re-written as

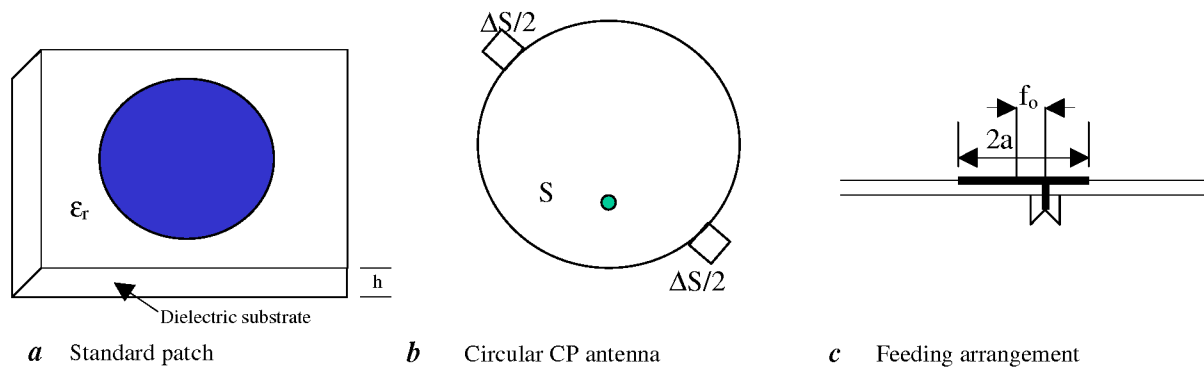


Figure 2. Patch and feed configuration of CP antenna.

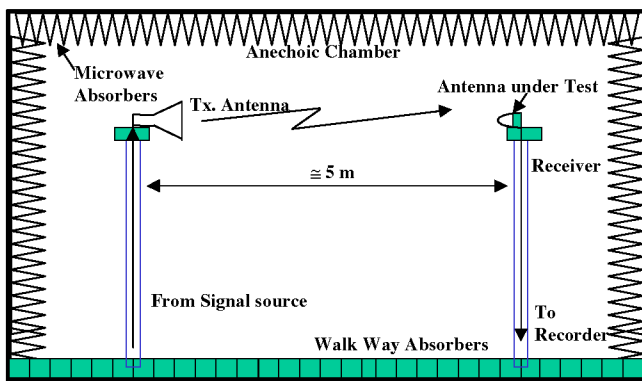


Figure 3. Experimental test set-up.

$$a_e = \frac{1.841}{k_0 \sqrt{\epsilon_r}} \quad (5)$$

For design of the antenna, the desired value of  $a_e$  at the operating frequency  $f_r$  is first obtained as (eq. (5))

$$a_e = \frac{8.794}{f_r \sqrt{\epsilon_r}} \quad (f_r \text{ in GHz}) \quad (6)$$

The relation between  $a$  and  $a_e$  is used to obtain the required value of  $a$  for a given substrate dielectric ( $\epsilon_r$ ), thickness ( $h$ ) and resonance frequency. A thicker substrate, besides being mechanically strong will increase the radiated power, reduce conductor loss and improve the impedance bandwidth. However, it will increase the weight, dielectric loss and extraneous radiations from the probe feed. The substrate dielectric constant  $\epsilon_r$  plays a role similar to that of substrate thickness. A low value of  $\epsilon_r$  will increase the fringing field at the patch periphery and thus the radiated power. Therefore, a substrate with  $\epsilon_r \leq 2.5$  is preferred unless a smaller patch size is desired. Keeping the above considerations and the availability, a substrate with  $\epsilon_r$  and  $h$  as 2.2 and 62 mills (1.6 mm) respectively, is selected for design of patch antennas. The patch diameters at  $L_1$

and  $L_2$  frequencies are calculated (eqs (5) and (6)) as 70 and 90 mm respectively. The feed location is finalized based on the impedance matching between coaxial connector of  $50 \Omega$  and the patch. Using this procedure two circularly polarized patch antennas at  $L_1$  and  $L_2$  are designed and fabricated on RT-5880 copper clad material using photolithography process. The patches are gold-plated to avoid the corrosion effects.

To mitigate the multipath occurring through small elevation angles ( $-5^\circ$  and  $+5^\circ$ ) below and above the horizon, vertical ground planes can be used. The size and weight of the vertical ground plane are small compared to flat ground plane for this design. Moreover, weight of the flat ground plane will add to the weight of the antenna and can create wind load problems. In designing the vertical ground planes, the half power beamwidth of the antennas and the angular region over which multipath rejection is necessary are considered. The use of vertical ground plane reduces the overall weight of the antenna. The height and diameter of ground plane for  $L_1$  antenna are calculated as 10 mm ( $\lambda_{L1}/20$ ) and 100 mm ( $\lambda_{L1}/2$ ) respectively. These values for the  $L_2$  antenna are 12 mm ( $\lambda_{L2}/20$ ) and 122 mm ( $\lambda_{L2}/2$ ). The ground planes are fabricated with aluminum alloy material to reduce the weight. The ground planes are embedded in hemispherical thin-wall GFRP radomes, which protect the antennas from environmental extremities.

When the antenna is covered with radome<sup>7</sup>, its performance should not deteriorate; even if it deteriorates, it should be minimum. This is achieved by proper selection of material, shape and configuration of the radomes. The material should have low electrical loss characteristics and at the same time have high mechanical strength. These two requirements are contradictory, which needs some compromise between them. Shape is another factor. If the radome is flat, there is a possibility of dust accumulation that increases dielectric losses. This problem can be overcome by choosing a hemispherical or conical shape. The disadvantage with conical shape is restricted field-of-view. The right choice is hemispherical shape. The main advantage of hemispherical shape is that it gives normal incidence for

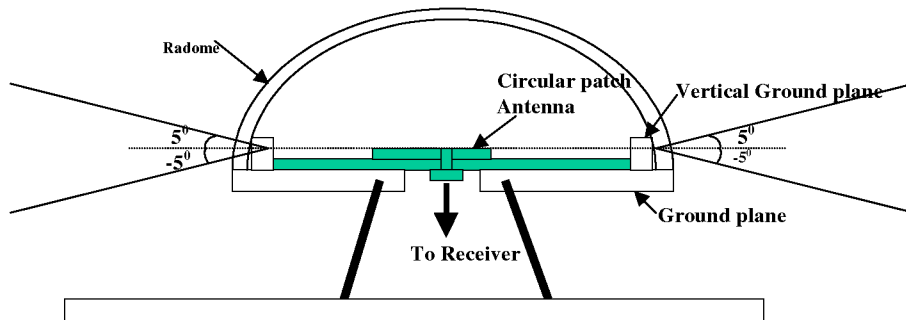


Figure 4. Mounting configuration of antenna with radome and vertical ground plane.

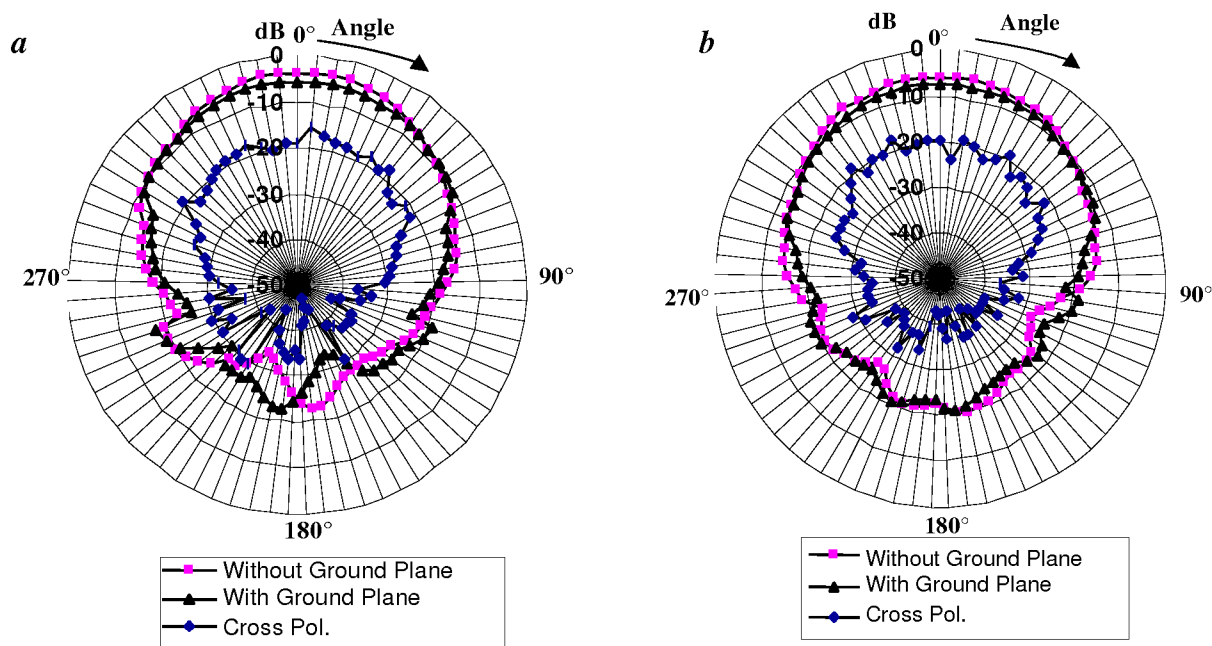


Figure 5. Typical radiation patterns of antennas including cross polarization patterns. *a*,  $L_1$  Frequency and *b*,  $L_2$  frequency.

all field-of-view angles. Electrically, a thin-wall configuration for radomes is better from the electromagnetic transparency point of view. The operating frequency and thickness are linearly related. Keeping the frequency of operation and its installation, the thin-wall configuration is chosen for radomes. The thickness of the thin-wall configuration is given as<sup>7</sup>

$$t = \frac{\lambda}{20\sqrt{\epsilon_r}} \tag{7}$$

where  $\lambda$  is the wavelength at operating frequency and  $\epsilon_r$  is the relative dielectric constant of the material used. The minimum thickness of a radome is calculated for an  $\epsilon_r$  of 6 at operating frequencies of  $L_1$  and  $L_2$  as 5.6 and 4.4 mm respectively (eq. (7)). If the thickness of a radome is less than the required value given in (eq. (7)), transmission loss will be reduced further. Since these radomes are for

ground platforms, the thickness is considered as 1 mm. The material used for fabrication of radomes is GFRP which is a combination of e(electrical)-glass cloth and epoxy resin. Hand-laying fabrication technique with female mould is adopted for fabrication of radomes.

Several radiation pattern measurements were made in an RF anechoic chamber. The experimental set-up along with the antenna mounting on receiving pedestal is shown in Figure 3. In this set-up the distance between the transmitting and receiving antenna is maintained as 5 m to fulfil the far-field criteria for plane wavefront. The transmitting antenna is under static condition, while the receiving antenna (i.e. antenna under test) is in movable condition on its own axis in different configurations to simulate different planes. Manual change of polarization of transmitting antenna at the transmitting end is possible. Initially radiation pattern of the antenna at the operating frequency is plotted on a polar chart by rotating the receiving antenna on its axis through 360°. Polarization of the transmitting antenna

is kept as vertical. The process is repeated when the antenna is covered with radomes along with ground plane. Radiation patterns are plotted using pattern recorder on the same chart for comparison. The whole process is carried out for both  $L_1$  and  $L_2$  antennas and for both polarizations.

Two circularly polarized circular patch antennas are designed and fabricated at  $L_1$  and  $L_2$  frequencies using RT-5880 substrate ( $\epsilon_r = 2.2$ ,  $h = 1.6$  mm) by adopting photolithographic process. Vertical ground planes are designed taking beamwidth of the antennas and cut-off angles for multipath rejection into consideration. GFRP radomes are designed to cover the antennas. The vertical ground planes are embedded into radomes to give more mechanical strength and firm fixing into the antenna. The mounting configuration of the antenna with radomes and vertical ground plane is shown in Figure 4. Return loss measurements of the antennas are carried out using network analyser and are found to be less than 20 dB at resonance frequencies of the two antennas. Radiation pattern measurements were carried out in an RF anechoic chamber for the two antennas (Figures 3 and 4). Initially, the radiation pattern of the antenna is plotted without the presence of the vertical ground planes and radomes. Later the ground planes and radomes are integrated with the antenna and the measurements were repeated. The patterns are superimposed on the same chart for easy comparison of the performance of the antenna with and without the presence of ground plane and radome. The typical radiation patterns of  $L_1$  and  $L_2$  antennas with and without the presence of ground planes and radomes are given in Figure 5. From the radiation pattern plots it is found that the transmission loss of the radome is 1 dB (90% transmission) for both the antennas. The half power beamwidth of the antenna in the presence of radome and ground plane increased by 10% (80 to 88° and 75 to 83° for  $L_1$  and  $L_2$  respectively). Variation in gain in the operating band is only 0.5 dB. Beam sharpening by 3 and 4 dB at the lower elevation angles for  $L_1$  and  $L_2$  respectively is achieved.

Various multipath rejection techniques are discussed and compared. A technique based on vertical ground plane is developed to reject multipath signals entering the GPS receiving antenna through low elevation angles above and below the horizon. The technique is validated with design and development of two circular patch antennas with vertical ground planes. Experimentation is carried out on these two circular polarized patch antennas at  $L_1$  and  $L_2$  frequencies with vertical ground planes and radomes. At low elevation angles ( $\pm 5^\circ$ ), beam sharpening takes place, which will help in rejecting multipath signals. Beamwidth of the antennas is improved significantly by 10%.

1. Parkinson, B. W. and Spilker, J. R., *Global Positioning System: Theory and Application*, American Institute of Aeronautics and Astronautics, Washington DC, 1996.
2. Hannah, B. M., Modeling and simulation of GPS multipath propagation, Ph D thesis, Queensland University of Technology, Australia, 2001.

3. Pasetti, A. and Glulichchi, L., Experimental results on three multipath compensation techniques for GPS-based attitude determination. American Astronautical Society (AAS 99-013), 3–7 February 1999.
4. Counselman, C. C., Multipath rejecting GPS antennas. *Proc. IEEE*, 1999, **87**, 86–91.
5. Bhal, I. J. and Bhartia, P., *Microstrip Antennas*, Artech House, New York, 1980.
6. Garg, R., Bhartia, P. and Inder Bahl, *Microstrip Antenna Design Hand Book*, Artech House, New York, 2001.
7. Walton, J. D., *Techniques of Radomes Design*, McGraw Hill, New York, 1970.

ACKNOWLEDGEMENTS. We thank G. Kumarswamy Rao, Director, DLRL for interest in this work. Thanks are also due to Dr V. Misra, for his constant encouragement.

Received 21 May 2005; revised accepted 3 November 2005

## Study of high-resolution satellite geoid and gravity anomaly data over the Bay of Bengal

T. J. Majumdar<sup>1</sup>, K. S. Krishna<sup>2,\*</sup>, S. Chatterjee<sup>1</sup>, R. Bhattacharya<sup>1</sup> and Laju Michael<sup>2</sup>

<sup>1</sup>Marine and Water Resource Group, Remote Sensing Applications Area, Space Applications Centre, Indian Space Research Organization, Ahmedabad 380 015, India

<sup>2</sup>Geological Oceanography Division, National Institute of Oceanography, Dona Paula, Goa 403 004, India

**Geoid and gravity anomalies derived from satellite altimetry are gradually gaining importance in marine geo-scientific investigations. Very high-resolution gravity database generated from Seasat, Geosat GM, ERS-1 and TOPEX/POSEIDON altimeters data of the northern Indian Ocean, has been used in the preparation of geoid and free-air gravity maps. In the present work, we have investigated various products of satellite data of the Bay of Bengal, thereby correlated to known plate tectonic feature (Sunda subduction zone), volcanic traces (Ninetyeast and 85°E ridges) and continental margin features. Besides, Swatch of No Ground and modified continental slope due to sediment discharge from East Coast rivers are some of the finer structures observed in free-air gravity anomaly data. Furthermore, the data are compared with ship-track gravity anomalies along 14.64°N lat. for their consistencies and interpreted under the constraints of seismic results for understanding the evolution of structural features of the region. Two different wavelength (100–200 and 200–500 km) components derived from satellite gravity anomaly data have been studied to explain the geophysi-**

\*For correspondence. (e-mail: krishna@nio.org)